ELECTRICAL RELAXATION IN PROTON CONDUCTOR COMPOSITES BASED ON $(NH_4)H_2PO_4/TiO_2$

J. Castillo [1], E. M. Materón [2], R. Castillo [2], R. A. Vargas [2], P.R. Bueno [3], J. A. Varela [3]*

- ✓ Este artículo forma parte del "Volumen Suplemento" **S1** de *la Revista Latinoamericana de Metalurgia y Materiales* (*RLMM*). Los suplementos de la RLMM son números especiales de la revista dedicados a publicar memorias de congresos.
- ✓ Este suplemento constituye las memorias del congreso "*X Iberoamericano de Metalurgia y Materiales (X IBEROMET)*" celebrado en Cartagena, Colombia, del 13 al 17 de Octubre de 2008.
- ✓ La selección y arbitraje de los trabajos que aparecen en este suplemento fue responsabilidad del Comité Organizador del *X IBEROMET*, quien nombró una comisión *ad-hoc* para este fin (véase editorial de este suplemento).
- ✓ La *RLMM* no sometió estos artículos al proceso regular de arbitraje que utiliza la revista para los números regulares de la misma.
- ✓ Se recomendó el uso de las "Instrucciones para Autores" establecidas por la *RLMM* para la elaboración de los artículos. No obstante, la revisión principal del formato de los artículos que aparecen en este suplemento fue responsabilidad del Comité Organizador del *X IBEROMET*.

Suplemento de la Revista Latinoamericana de Metalurgia y Materiales 2009; **S1** (2): 449-459

ELECTRICAL RELAXATION IN PROTON CONDUCTOR COMPOSITES BASED ON $(NH_4)H_2PO_4/TiO_2$

J. Castillo [1], E. M. Materón [2], R. Castillo [2], R. A. Vargas [2], P.R. Bueno [3], J. A. Varela [3]*

1: Programa de Física, Universidad del Quindío, Armenia, Colombia.
2: Departamento de Física, Universidad del Valle, A.A. 25360, Cali, Colombia.
3: Departamento de Físico-Química, Instituto de Química, Universidade Estadual Paulista, P.O. Box 355, 14800-900, Araraquara, São Paulo, Brazil.

** E-mail: jocacha8@gmail.com*

Trabajos presentados en el X CONGRESO IBEROAMERICANO DE METALURGIA Y MATERIALES IBEROMET
Cartagena de Indias (Colombia), 13 al 17 de Octubre de 2008
Selección de trabajos a cargo de los organizadores del evento

Publicado On-Line el 29-Jul-2009
Disponible en: *www.polimeros.labb.usb.ve/RLMM/home.html*

Abstract

Admittance measurements were used to study electrical relaxation in $(1–x)(NH_4)H_2PO_4–xTiO_2$ ($x \leq 0.1$) composites. Three different phases are identified: (I) from 303 to 373 K, followed by mid- and high-temperature regions (II, 373<T≤523 K and III, T >523 K, respectively). The real part conductivity, , is well described by the Jonscher's expression $\sigma(\omega) = \sigma_0(1 + (\omega/\omega_p)^n) + A\omega$, where σ_0 is the *dc*-conductivity, $\omega p/2\pi=f_p$, is a characteristic relaxation frequency, $n= \beta$-1 is a fractional exponent between 0 and 1, and A is an constant. Both σ_0 and f_p are equally thermal activated in the region II indicating that the dispersive conductivity originates from migration of protons. We have observed that the conductivity relaxation in these composites is highly non-exponential (β =0.61), which is independent of temperature but depends on composition.The highest dc-conductivity is obtained for the concentration x=0.05, which about 3 orders of magnitude higher that that of crystalline ADP, reaching values of the order of 0.1 $(\Omega cm)^{-1}$ above 523 K. The enhancement of conductivity in the composites is attributed to thestructural disorder in the interfaces of nanoparticles with the ADP solid matrix. The results confirm the dehydration reactions in the composites above T_p=460 K, as previously suggested for pure ADP.

Keywords: *Protonic composites, Phase behavior, Electrical relaxation*

Resumen

Medidas de admitancia fueron usadas para estudiar relajación eléctrica en $(1–x)(NH_4)H_2PO_4–xTiO_2$ compositas. Se identificaron tres fases diferentes: (I) desde 303 hasta 373 K, seguida por regiones intermedias y a altas temperaturas (II, 373 < T ≤ 523 y III, T > 523 K, respectivamente). La parte real de la conductividad, σ', se describe bien por la expresión de Jonscher $\sigma(\omega) = \sigma_0(1 + (\omega/\omega_p)^n) + A\omega$, donde σ_0 es la conductividad *dc*, $\omega p/2\pi=f_p$, es una frecuencia de relajación característica, $n=\beta$-1 es un exponente fraccionario entre 0 y 1, y A es una constante. Tanto σ_0 como f_p están igualmente activadas en la región II indicando que la conductividad dispersiva se origina de la migración de protones. Hemos observado que la relajación de la conductividad en estos compositos es altamente no exponencial (β=0.61), la cual es independiente de la temperatura pero depende de la composición. La más alta conductividad dc se obtiene para la concentración x=0.05, que es alrededor de 3 ordenes de magnitud más alta que el ADP cristalino, logrando valores del orden de 0.1 $(\Omega cm)^{-1}$ por encima de 523 K. El incremento de la conductividad en las compositas es atribuida al desorden estructural en la interfase de las nano partículas con la matriz sólida del ADP. Los resultados confirman las reacciones de hidratación en las compositas por encima de T_p=460K, como se sugirió previamente para el ADP puro.

Palabras claves*: Compositas protónicas, Comportamientos de fases, Relajación eléctrica*

1. INTRODUCTION

Ammonium dihydrogen phosphate (ADP), $(NH_4)H_2PO_4$, is an interesting material and, due to that fact, several research workers have shown considerable interest on it (Davey and Mullin; Levina and Belyustin; Nagalingam et al; Ramesh and Mahadevan) [1–4]. The electrical conduction in dielectrics is mainly a defect controlled process in

the low temperature region. The presence of impurities and vacancies mainly determine this region. The energy needed to form the defect is much larger than the energy needed for its drift. The conductivity of the crystal in the higher temperature region is determined by the intrinsic defects caused by thermal fluctuations in the crystal (Freeda and Mahadevan) [5].

The electrical conduction in $(NH_4)H_2PO_4$ crystals can be understood as due to proton as in the case of KH_2PO_4. The conduction is mainly due to the anions dynamics, viz. $(H_2PO_4)^{-1}$ ions (Freeda and Mahadevan; Priya et al; Sancta et al; Deepa et al) [5–8]. Electrical conductivity may be explained by the proton transport within the framework of hydrogen bonds. The conductivity is associated with the incorporation into the crystal lattice of impurities and the formation of corresponding defects in ionic crystals. The proton conduction may be accounted for by motion of protons accompanied by a D defect (excess of positive charge). Migration of these defects may only modify electric polarization and may not change the charge at an electrode [5]. The motion of defects occurs by some kind of rotation in the bond with defects. The speed of displacement, $v \approx \nu a$, where a and ν are the distance and frequency, respectively of the jump from one bond to the other.

The high-temperature phase transition of KDP crystal was suggested to occur at a temperature close to the onset of thermal decomposition. Since the interpretation of the experimental evidence of the HTPT is impeded by the crystal decomposition, there were many controversies about the existence and nature of the HTPT. Based on chemical analysis, many researches have proposed that partial thermal decomposition sets in around T_p, corresponding to the following dehydration reaction [9–17]:

$$nMH_2XO_4(s) \rightarrow M_nH_2X_nO_{3n+1}(s) + (n-1)H_2O(v) \quad n \geq 1 \quad (1)$$

and claimed that the term HTPT should be repalced by the onset of partial polymerization at reaction sites on the surface of the crystal. Here n is the number of molecules participating in the thermal decomposition. The letter s or v enclosed in parentheesis denotes that the corresponding compound is in the solid or vapor state, respectively.

Especially, macroscopic observations such as electrical conductivity and dielectric constant, which are greatly dependent upon defect states due to dehydration, could not give clear evidences of the HTPT. Recently, it was found from Raman scattering measurements that KDP crystal undergoes two successive HTPTs at around 468 and 488 K, after the onset of thermal decomposition near 448 K [18]. The thermal decomposition could be much suppressed by using a glass seal.

As ionic conduction is facilitated by structural disorder, we have studied the high-temperaure phenomena and the dynamics of mobile protons in ADP–based composites, since proton trasport may be affected by the presence of outer and inner surfaces provided by highly dispersed ceramic nanoparticles, such as TiO_2 in the ADP solid matrix.

2. EXPERIMENTAL

The different samples were sintered from $NH_4H_2PO_4$ 99.999% powder, (Aldrich) and TiO_2 nanoparticles powder (99.8% trace metal basic) (<100nm (BET), <50nm (XRD)). Composites with compositions $(1–x)NH_4H_2PO–xTiO_2$ were investigated, where x, the mole ratios of heterogeneous components TiO_2, were varied in the range from 0 to 0.1. The composites were prepared by thoroughly mixing the component in an agate mortar and then heated for 2 hours at 423 K close to the reported dehydration reaction of ADP.

Differential scanning calorimetry (DSC) was performed with a TA instruments 2920 Modulated DSC with a temperature scan of 10 K/min and under a dry N_2 flux.

The electrical characterization of the samples was done by impedance spectroscopy (IS) using a two electrode configuration Pt|sample|Pt and a home-built temperature and atmosphere controlled cell for measurements. The electrode-electrolyte contact surface (A) and the distance between electrodes (d) were measured using a micrometer. No corrections for thermal expansion of the cell were carried out. The measuremets were carried out with a computer controlled Agilent 4294A LCR meter in the frequency range of 40 Hz -13 MHz, in the isothermal or in the heating cooling modes, at temperatures between $303 \leq T \leq 553$ K in air.

From the admittance data, $Y(\omega)=Z^{-1}(\omega)=G(\omega)+i\omega C(\omega)$ (where $\omega = 2\pi f$ / Hz is the angular frequency, $i = \sqrt{-1}$, G and C, the parallel conductance and capacitance, respectively), the real part of the electrical conductivity,

$\sigma'(\omega) = (d/A)G(\omega)$, was obtained. It is important to point out that $\sigma(\omega) = (d/A)Y(\omega) = \sigma'(\omega) + i\sigma''(\omega)$ is the preferred quantity to represent the behavior of conducting materials [19-25]. In terms of the impedance data,

$$\sigma'(\omega) = (d/A)G(\omega) = \frac{d}{A}\frac{Z'}{(Z'^2 + Z''^2)}, \qquad (2)$$

Similarly, the dielectric permittivity data as function of frequency is calculated from,

$\varepsilon(\omega) = \frac{\sigma(\omega)}{i\omega\varepsilon_0}$, where ε_0 is the permittivity of free space, such that, the real and imaginary part of the dielectric permittivity in terms of the impedance data,

$$\varepsilon'_r = \frac{d}{\omega A \varepsilon_0}\left[\frac{-Z''}{Z'^2 + Z''^2}\right] \qquad (3)$$

$$\varepsilon''_r = \frac{d}{\omega A \varepsilon_0}\left[\frac{Z'}{Z'^2 + Z''^2}\right] \qquad (4)$$

where Z' and Z'' are the real and imaginary part of the impedance.

3. RESULTS AND DISCUSSION

Fig. 1 shows the DSC first heating curve (solid line) for the $0.975NH_4H_2PO_4$–$0.025TiO_2$ composite in the $233 \leq T \leq 623$ K temperature range and the temperature dependence of its conductivity at a fixed frequency of 204 Hz, for comparison. The conductivity data was recorded during the first heating run at a rate of 10 K/min in air, using a sample from the same batch as that for the DSC measurements. At this first heating run, the conductivty decreases with increasing temperature in the 303-373 K temperature range due to moisture traces at the sample surface. This behaviour is correlated with a small endothermic anomaly observed in the DSC curve in the same temperature region (see inset in Fig. 1). These observations may correspond to the earlier conductivity measurements found a knee at around 360 K in the conductivity curve, which was attributed to a structural phase transition for pure ADP at about the same temperatures [26, 27]. On further heating the sample under the same conditions, the conductivity increases monotonically with increasing temperature up to 523 K, where an abrupt step change to higher values (of about two order of magnitude) is observed. However, above 463 K a lower variation of the conductivity with temperature is apparent. In concordance with these transition temperatures, the DSC curve shows a double peak anomaly at around 463 K, the first one being endothermic with an onset temperature at about 450 K, followed by an exothermic one at higher temperature. It is also clear an additional exothermic peak whose onset temperature is at 523 K, where the step change in the conductivity curve is observed.

The electrical response of ion-conducting disordered solids, are characterized in the frequency domain by dispersion in the conductivity or the permittivity spectra. Fig. 2 shows the Nyquist plots, *-ImZ vs. ReZ*, for the impedance behavior of the $0.975(NH_4)H_2PO_4$–$0.025TiO_2$ composite at selected temperature 443 K. In this temperature range, typical spectra consist of two parts: (i) a high-frequency non-ideal semicircle, whose center is displaced below the real axis, due to the bulk response of the sample, and (ii) a low-frequency linear variation due to the sample-electrode interface.

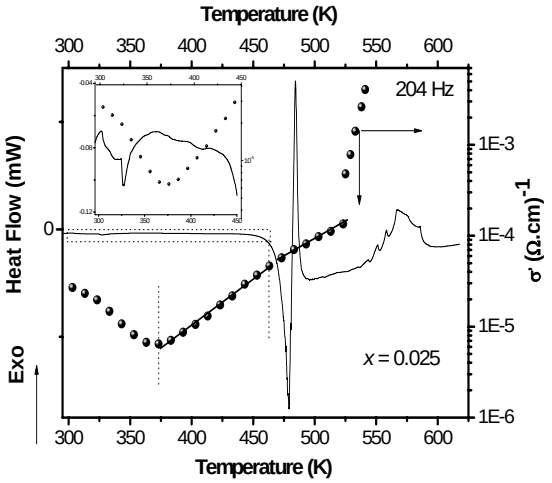


Fig. 1. Temperature dependence of the ionic conductivity σ' at a frequency of 204 Hz (full circles) and DSC heat flow (solid line) for the $0.975(NH_4)H_2PO_4$–$0.025TiO_2$ composite. The inset shows the region around 350 K on an amplified scale.

Formalisms such as electric conductivity, electric modulus and electric permittivity [28–31] have been employed to study the ion dynamics in glasses under ac electric field. However, there is a debate on

which of the formalisms provides better insights into the phenomena of ion dynamics [32–34]. In this work, we have studied the ionic relaxation in the $(1–x)(NH_4)H_2PO_4–xTiO_2$ ($x \leq 0.1$) composites in the framework of the three formalisms, i.e. the conductivity relaxation mechanism. In the permittivity formalism [35], an electric permittivity ε^* is defined as, $\varepsilon^*(\omega) = \varepsilon'(\omega) - i\varepsilon''(\omega)$, where ε' and ε'' are the real and imaginary part of the permittivity ε^*. The complex dielectric permittivity may be expressed by the superposition relation [35, 36]:

$$\frac{\varepsilon^*(\omega) - \varepsilon_\infty}{\varepsilon_0 - \varepsilon_\infty} = \int_0^\infty \left[-\frac{d\phi(t)}{dt} \right] e^{-i\omega t} dt \qquad (5)$$

ε_0 and ε_∞ are the limiting low and high frequency dielectric permittivities respectively. $\phi(t)$ is the normalized decay function obtained on the removal of a steady electric field from a sample contained in a parallel plate capacitor. $\phi(t)$ involves only relaxation, and omits the instantaneous decay due to deformation polarization.

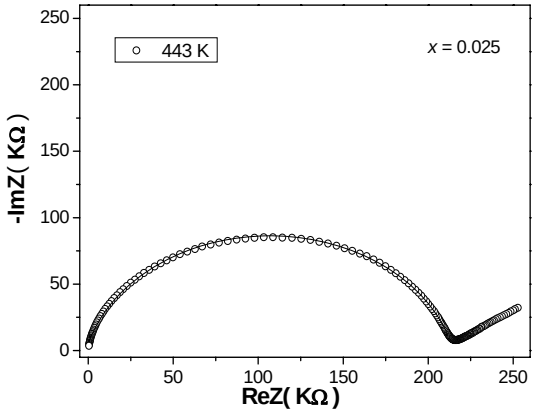


Fig. 2. Typical impedance spectra for the $0.975(NH_4)H_2PO_4$-$0.025TiO_2$ composite at temperature the 443 K. The solid lines are fitting circular arc representing model circuits.

In the modulus formalism [37–38], an electric modulus M^* is defined as the inverse of the complex dielectric permittivity ε^*:

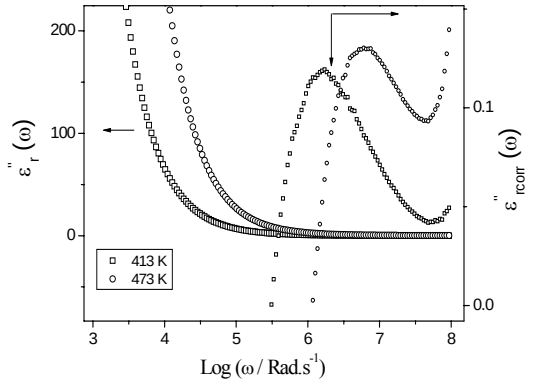
$$M^*(\omega)\varepsilon^*(\omega) = 1$$

$$M'(\omega) = \frac{\varepsilon'(\omega)}{\varepsilon'^2(\omega) + \varepsilon''^2(\omega)} \quad \text{and}$$

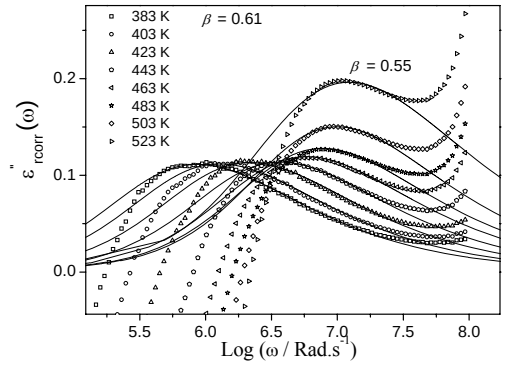
$$M''(\omega) = \frac{\varepsilon''(\omega)}{\varepsilon'^2(\omega) + \varepsilon''^2(\omega)}$$

$$M^*(\omega) = M_\infty \left[1 - \int_0^\infty -\frac{d\phi(t)}{dt} \exp(-i\omega t) dt \right] \qquad (6)$$

Where M' and M'' are the real and imaginary part of the complex modulus M^* and M_∞ is the high frequency value of M'.



(*a*)



(b)

Fig. 3 (*a*) Typical frequency dependence of the imaginary part of permittivity data, ε_r'' and ε_{rcorr}'', before and after subtracting the dc-conductivity contribution, for the $0.975(NH_4)H_2PO_4–0.025TiO_2$ composite. (b) ε_{rcorr}'' at different temperatures. The continuous line represents the fits of Eq.(5) to the experimental data for ε_{rcorr}''

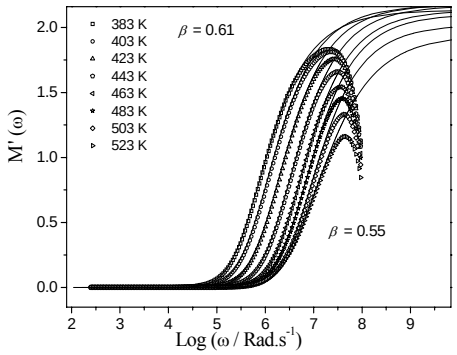
Fig 3(*a*) shows the typical variation of the imaginary part of permittivity, ε_r'', as a function of frequency for $(1–x)(NH_4)H_2PO_4–xTiO_2$ (x = 0.025) at 413 and 473 K, respectively. The ε_r'' value is found to increase with temperature. In the case of solid electrolytes, the total dielectric loss has two contributions: (i) dipole relaxation loss, and (ii) conduction loss. In fast ion conductors with appreciable dc-conductivity, the relaxation from the polarization of mobile-charged species present in the material suppresses the dielectric relaxation peaks due to permanent or induced dipoles. To obtain true dielectric relaxation loss as a function of frequency at different temperatures, the usual procedure is to subtract the *dc*-conductivity contribution of the loss $\frac{\sigma_0}{\omega\varepsilon_0}$ from the total dielectric loss ε_r''. The corrected dielectric relaxation spectra is show in Fig. 3(*a*) along with the ε_r'' plot, which shows that the contribution from dipole relaxation loss is much smaller compared to ε_r''.

The frequency dependence of the corrected imaginary part of the relative permittivity (after subtracting the dc-conductivity contribution), of $(1-x)(NH_4)H_2PO_4–xTiO_2$ (x = 0.025) composites is show in Fig. 3(b) for various temperatures. Well-defined peaks in the ε''_{rcorr} versus log(ω) plots are observed in Fig. 3(b) corresponding to dielectric relaxation phenomena, the position of the peak shifts to higher frequency with increasing temperature, indicating a thermally activated process. In the corrected imaginary part of the relative permittivity curves, the continuous line represents the fits of Eq.(4) to the experimental data for ε''_{rcorr}, whereas the symbols correspond to the experimental data of the composites. In the fitting process, we have used the non-exponential Kohlrausch-Williams-Watts (KWW) function [36]

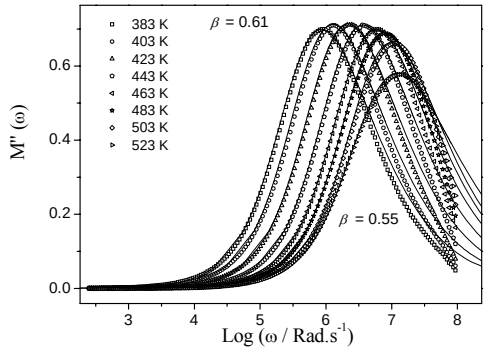
$$\Phi(t) = \exp\left(-\left(t/\tau\right)^{\beta}\right) \qquad (7)$$

where $0 < \beta < 1$ is an exponent indicating departure from the Debye relaxation (β = 1) and τ is the characteristic relaxation time.. It was observed that values of β were almost independent of temperature. These values of β indicate that the conductivity relaxation is highly non-exponential at temperatures between 383 and 523 K.

Fig. 4 (*a*) and (b) show the real and imaginary part of electric modulus versus the angular frequency; spectra plotted at different temperatures for $(1–x)(NH_4)H_2PO_4–xTiO_2$ (x = 0.025) composites. In the modulus curves, the continuous line represents the fits of Eq.(6) to the experimental data for M' and M'', whereas the symbols correspond to the experimental data of the composites. Also in the fitting process we have used the non exponential Kohlrausch-Williams-Watts (KWW) function [36]



(*a*)

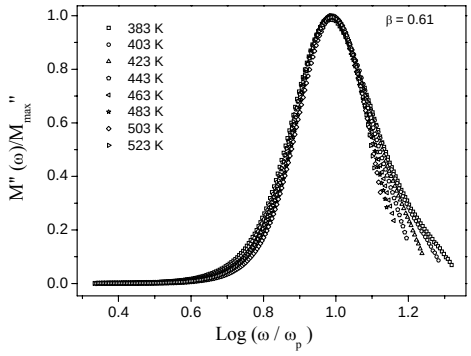


(b)

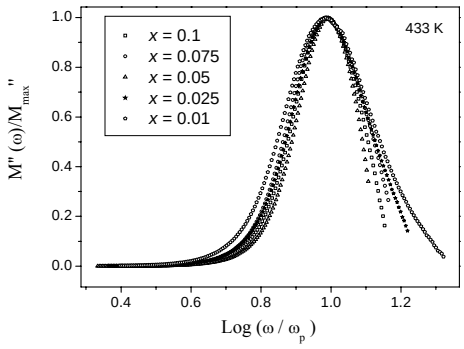
Fig. 4. Frequency dependence of (*a*) the real part, $M'(\omega)$ and (b) the imaginary part, $M''(\omega)$, of the electric modulus at different temperatures. The continuous line represents the fits of Eq.(6) to the experimental data for $M'(\omega)$ and $M''(\omega)$, repectively.

Fig. 4(*a*) shows that real modulus M' shows dispersion as the frequency is increased and tends to decrease at higher frequencies. The imaginary

modulus M'' [Fig. 4(b)] exhibits a maximum $M''_{\max}$ centered at the dispersion region of M'. However, it is observed that with temperature, $M''_{\max}$ value remains constant and the position of the peak frequency shifts towards the higher frequency region. The conductivity relaxation frequency ω_p corresponding to $M''_{\max}$, gives the most probable conductivity relaxation time τ_p by the condition $\omega_p \tau_p = 1$ [37].



(*a*)



(b)

Fig. 5. Plots of (a) $M''/M''_{\max}$ versus $\log(\omega/\omega_p)$ at different temperatures for $0.975(NH_4)H_2PO_4$–$0.025TiO_2$, and (b) $M''/M''_{\max}$ versus $\log(\omega/\omega_p)$ for a fixed temperature (433 K) and different mole ratios (*x*).

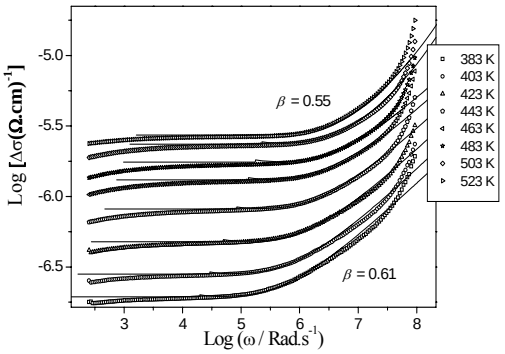
The spectra for $M''(\omega)$ at different temperatures for a representative $0.975(NH_4)H_2PO_4$–$0.025TiO_2$ composite have been scaled in Fig 5(a). In the scaling process $M''(\omega)$ are scaled by $M''_{\max}$, while the frequency axis is scaled by the relaxation frequency ω_p. We observe that the spectra for $M''(\omega)$ for different temperatures merge on a single master curve. Thus, the dynamical processes occurring at different temperatures are independent of temperature. Such results were also observed for other compositions. Moreover, the value of the parameter β, determined from the full width at half maximum of the modulus spectra in fig. 4, was found to be independent of temperature with an value of 0.61. This value of β clearly indicates that the relaxation is non-exponential.

Now it is interesting to note the composition dependence of the scaling behavior of the modulus spectra. In Fig. 4(b) we have shown the scaled spectra for $M''(\omega)$, for different compositions at a fixed temperature (433 K). It is noted that the spectra for different compositions do not merge on a single master curve, which implies that the conductivity relaxation depends of the mole ratios of heterogeneous components TiO_2.

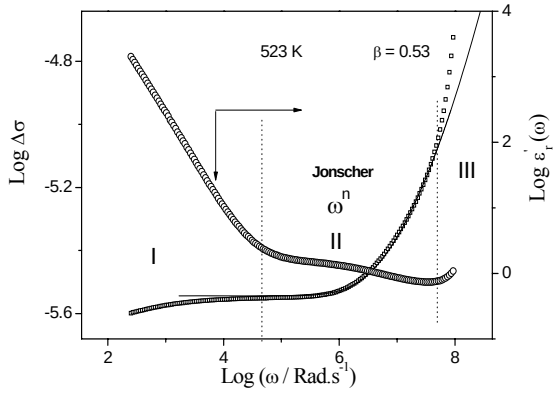
The *dc* bulk conductivity can be analyzed by means of the impedance (*Z*) or the admittance (*Y*) formalisms [19–24]. Using the impedance data (Fig.2), the bulk resistance of the sample, *R*, is calculated from the intersection with the real axis of the circular arc fitted to the high-frequency part of the espectra. Solid lines in Fig. 2 represent the best fitting arcs to these parts of the spectra. From these values, the *dc*-conductivity data were calculated from, $\sigma_0 = \frac{d}{RA}$, where *A* is the electrode-electrolyte contact surface and *d* the distance between electrodes. The *dc*-conductivity data obtained by this formalism is presented below, together with those obtained by the admittance formalism (see Fig. 7(*a*)).

Fig. 6(*a*) shows typical plots of the angular frequency dependence of the real part of conductivity, $\Delta\sigma(\omega) = \sigma'(\omega) - \sigma_0$, at several isotherms between 383 and 524 K for a representative non-treated $0.975(NH_4)H_2PO_4$–$0.025TiO_2$ composite. At low temperatures (T<524 K) and frequencies higher than about 10^3 Hz, $\Delta\sigma(\omega)$, shows a medium-frequency plateau which is associated with the bulk *dc*-conductivity of the sample at temperature $T, \sigma_0(T)$ [22–24]. As temperature T is increased, the values $\sigma_0(T)$ increase. For a fixed temperature, $\Delta\sigma(\omega)$ increases

with increasing frequency after a characteristic crossover frequency, $\omega_{p,}$, that also increases with temperature. These curves also show an additional low frequency dispersive region ($f < 10^3$ Hz) which is attributed to the electrode-sample interface polarization. In addition, the impedance behavior at the low frequency region is observed to be more dominant in the 525 K isotherm curve. These profiles are in accordance with previous studies on other ionic conductors [19–24].



(*a*)



(b)

Fig. 6. Frequency dependence of the real parts of the (*a*) conductivity, $\Delta\sigma$, at temperatures between 383 and 524 K, for the $0.975(NH_4)H_2PO_4$–$0.025TiO_2$ composite. The solid lines represent fitting curves to the Eq. (6) with β = 0.53, and (*b*) conductivity and permittivity at 523K, for the same composite.

The conductivity $\Delta\sigma(\omega)$ caused by ionic displacements (hops) are higher at high frequencies than at low ones, because more ionic hops are seen per unit time when the experimental time window, f^{-1}, is short than when it is long. Thus, $\Delta\sigma$, is found to be frequency independent in the low frequency region ($\omega < \omega_p$) because the ion diffusion is more correlated, i.e., the ions perform correlated forward-backward motions [19-23]. This relaxation process is fast at high temperatures, but slow at low temperatures. Consequently, the crossover frequency, ω_p, at which the conductivity attains, is dc plateau is found to decrease with decreasing temperature, Fig. 7.

Conductivity spectra of ion-conducting materials, taken at a fixed temperature, are often found to increase at high frequencies according to a power law, $\Delta\sigma \sim \omega^n$, where $n = 1-\beta$ is a fractional exponent between 0 and 1. The parameter n has been proposed to be close to 1 for strongly correlated ion motion and equals to 0 for completely random and independent Debye-like ion hops [28, 33, 39]. It is usual to express $\sigma'(\omega)$ as the empirical Jonscher power law [28]

$$\sigma' - \sigma_0 = \Delta\sigma = \sigma_0\left[\left(\omega/\omega_p\right)^n\right] + A\,\omega \qquad (8)$$

where σ_0 is the dc-conductivity, and $\omega_p/2\pi$ is a characteristic relaxation or crossover frequency, f_p. For the plots shown in Fig. 6(*a*), the solid lines are fitting curves to Eq. (8).

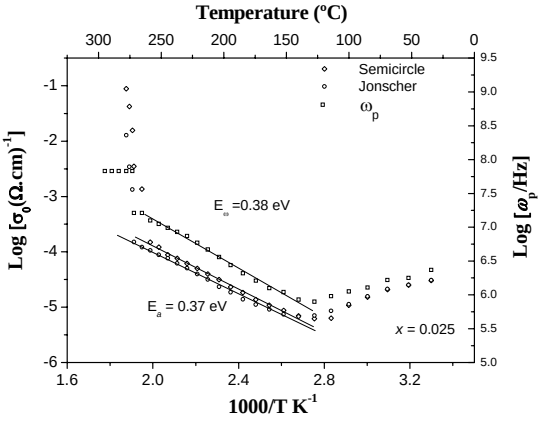


Fig.7. Arrhenius plots of the temperature dependence of the dc-conductivity, σ_0, and the crossover frequency, ω_p, for the $0.975(NH_4)H_2PO_4$–$0.025TiO_2$ composite, obtained using the circuit models (◊ symbols) and the Jonscher's expression (7) (o symbols). The solid straight lines are least square fittings to a segment of data points (373<T<523 K, for σ_0 and ω_p).

On the other hand, in order to allow accurate assesment of the quality of the empirical Jonscher power law (8) predictions, a representative isotherm impedance data at high-temperature (523 K) are plotted in Fig. 6(*b*) as real parts of conductivity, $\Delta\sigma(\omega)$, and permittivity, $\varepsilon_r'(\omega)$, respectively. In both representations, it is clear at this isotherm the presence of three regimes of ionic motion: (i) regime I occur at low-frequencies (less than 20 kHz) which corresponds to the ionic processes at the sample-electrode interface. The increase of the real part of the permittivity with decreasing frequency is attributed to the accumulation of charge at the interface and the net polarization capacitance resulting from the formation of a region of space charge at the electrode-electrolyte interface. (ii) Regime II occurs at intermediate frequencies (20 kHz $\leq f \leq$ 4.21 MHz), which corresponds to the bulk response of the sample. For this region, the conductivity data can be fitted to the Jonscher's equation (8). The solid line in Fig. 6(*b*) is the fitting curve to Eq. (8). The fitting parameters σ_0, $\omega_p/2\pi$, obtained at various isotherms are presented in Arrhenius form in Fig 7. The corresponding permittivity data in this intermediate frequency regime also decrease lineraly with increasing frequency but with slower slope that that shown in the low-frequency regime. The presence of this second dispersive region in the permittivity curve indicates that there is a bulk polarization resulting from induced dipolar moments due to shifting of molecules when electric field is applied. (iii) Regime III occurs at high frequencies (above 4.21 MHz), which is evident for different temperatures, where both conductivity and permittivity grow rapidly with frequency (while the real part of the electric modulus, M', decreases at higher frequencies), which might be due to a much faster polarization process occurring in the material.

It is clear from Fig. 7, where the dc-conductivity data obtained either using the equivalent circuit analysis for the impedance (*Z*) plots (Fig. 2) or the fitting of the admittance plots (Fig. 6) to Eq. (8), that both methods are equivalent. Thus, $\sigma = (d/A)Y(\omega) = \sigma'(\omega) + i\sigma''(\omega)$ is the preferred quantity to represent the behavior of conducting materials without any use of equivalent circuit analysis, as discussed in references [19–24]. Based on least square analysis of the σ_0 data, straight lines fit well both Arrhenius plots, if an intermediate temperature segment of each data plot is selected (from about 373 to 523 K). The activation energy, E_a, was calculate from the fitting parameter to the Arrhenius model, $\sigma_0 = \Gamma \exp\left(-E_a/kT\right)$, where Γ is the preexponential factor, *k* is the Boltzmann constant and *T* the absolute temperature. Activation energies of the order of 0.37 eV were obtained from both dc-conductivity plots. Similar results are obtained for the Arrhenius plot of the crossover frequency, $\omega_p = \omega_0 \exp\left(-E_\omega/kT\right)$.

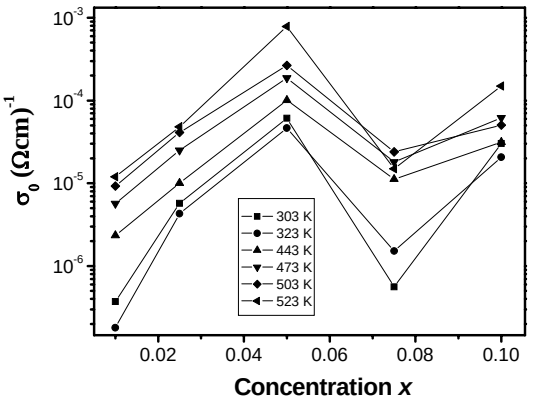


Fig. 8. Concentration dependence, *x*, of the dc-conductivity, σ_0, for the (1–x)$(NH_4)H_2PO_4$–*x*TiO_2 composites at temperatures between 303 and 523 K.

The fitting parameter E_ω was almost equivalent to E_a parameters obtained from the dc-conductivity data, e.g., 0.38 eV.. These observations thus suggest that both long range transport conductivity (non dispersive behavior, σ_0) and mobile ion relaxation, $G(\omega) \sim \omega^n$, have common origin. In other words, these observations confirm that a common charge transfer mechanism based on ion migration mediated by either ion-ion or ion-lattice interactions are responsible for ionic conductivity in the 383–523 K temperature range. Notice that above 463 K, the DSC results (Fig. 1) indicate a different composite phase or the presence of a second hydrated polyphosphate phase besides the ADP phase, according to the reaction (1). At 523 K, an abrupt change to higher values on both σ_0 and ω_p data is observed. This transition temperature corresponds to the exothermic peak shown by the DSC curve (Fig 1), where presumably a hydrated

Kurrol's salt C [9–17] is formed.

At this stage, the sample has a milky-white color with a gel-type consistency that diffuses easily in the metal electrodes and glass containers. This sample's appearance is kept when it is cooled to room temperature under an air atmosphere.

Table 1. Fitting parameters Ea, Eω, to the Arrhenius equation $\log K(T) = \log K_0 + E_a/k_BT$ for the *dc*-conductivity and crossover frequency data of the (1–x) $(NH_4)H_2PO_4$–xTiO_2 composites.

Concentration	*Region (373 < T ≤ 523 K) (Δea = ± 0.01). dc-conductivity*		*crossover frequency* ω_p
X	*Ea(eV). circuit model (ΔEa=±0.01)*	*Ea(eV), Jonscher's (ΔEa=±0.01)*	*Eω(eV) Jonscher's (ΔEω=±0.01)*
0.010	0.51	0.50	0.49
0.025	0.37	0.38	0.38
0.050	0.34	0.34	0.35
0.075	0.31	0.31	0.32
0.100	0.36	0.37	0.36

On the other hand, a low-temperature region from 300 to 373 K is also evident in Fig. 7, where both σ_0 and ω_p decreases with increasing temperature, following the same trend as a function of temperature. This behavior can be due to moisture traces at the sample surface enhancing proton transfer, such that again long range transport conductivity and mobile proton relaxation have common origin for this surface conduction.

As it is shown that σ_0 goes through a maximum, which takes place for the composite with x =0.05.

Identical results as those reported for the composite with x = 0.025 were found for the composites with x = 0.01-0.1 compositions of TiO_2 fillers and the corresponding fitting parameters are summarized in Table 1. It is found that the both activation energies, E_a and E_ω, decrease with increasing concentration up to x = 0.075. *dc*-conductivity isotherms as a function of TiO_2 mole ratio are presented in Fig. 8.

The best *dc*-conductivity in the intermediate temperature region is about 2.5 orders of magnitude higher than that of pure ADP. The increase in the dc conductivity and the corresponding decrease in the activation energies E_a and E_ω with increasing concentration for $x \leq 0.05$, might be due to the formation of H-bond defects at the interfaces between the ADP solid matrix and the TiO_2 nanoparticles, thus increasing rapidly the proton conductivity. Similar behavior of the *dc*-conductivity in KDP and ADP composites using urea and thiourea as ceramic fillers have been reported [44].

4. CONCLUSION

Our results, based on thermal analysis (DSC) and electrical relaxation measurements, indicate that the phase behavior of $(NH_4)H_2PO_4$ is very sensible to thermal treatments and points defects that can be modified by adding non-reactive ceramic particles such as TiO_2. For the $(NH_4)H_2PO_4/TiO_2$ composites, the activation energies associated with ion transport and the crossover frequency for electrical relaxation decrease from 0.49 eV to 0.32 eV as the concentration of the nanoparticles of TiO_2 increases. The highest dc-conductivity is obtained for the composite with concentration x=0.05, with a value at room temperature of 6.12×10^{-5} $(\Omega cm)^{-1}$, which is about 3 orders o magnitude higher that that of crystalline ADP, and rapidly increase with increasing temperature, reaching a value of the order of 0.1 $(\Omega cm)^{-1}$ above 523 K. The results show that all the transport parameters (exponent, β, the crossover frequency, ω_p, the dc-conductivity, σ_0) decrease with increasing temperature up to 373 K, where the DSC curve shows a small endothermic peak. This behavior may be associated with a dehydration process on the surface of the sample, such that, at 373 K, this reaction is completed. This region is followed by a stable phase up to 523 K in which the dc-conductivity and the crossover frequency are equally activated, indicating similar mechanism (ion jumping) for both processes. We have observed that the conductivity relaxation in these composites is highly non-exponential. The

conductivity relaxation is independent of temperature but depends on composition. Finally, above 523 K a highly conducting phase is found which will be subject of a future investigation.

5. REFERENCES

[1] R. J. Davey and J. W. Mullin 1976 Krist. Technol. **11** 22.

[2] I. M. Levina and A. V. Belyustin 1980 Soviet Phys. Cryst. **25** 209.

[3] S. Nagalingam, S. Vasudevan and P. Ramasamy 1981 Cryst. Res.Technol. **16** 647.

[4] R. Ramesh and C. Mahadevan 1998 Bull. Mater. Sci. **21** 287.

[5] T. H. Freeda and C. Mahadevan 2000 Bull. Mater. Sci. **23** 335.

[6] M. Priya, C. M. Padma, T. H. Freeda, C. Mahadevan and C. Balasingh 2001 Bull. Mater. Sci. **24** 511.

[7] J. A. Sancta, A. G. Sutha, T. H. Freeda, C. Mahadevan and C. Balasingh C 2001 Indian J. Phys. **A75** 245

[8] G. Deepa, T. H. Freeda and C. Mahadevan 2002 Indian J. Phys. **A76** 369.

[9] J. Grunberg, S. Levin, I. Pelah and E. Wiener, Solid State Commun. **5**, 863 (1967).

[10] M. O'Kee_e and C. T. Perrino, J. Phys. Chem. Solids **28**, 211 (1967).

[11] R. Blinc, V. Dimic, D. Kolar, G. Lahajnar, J. Stepisnik, S. Zumer, N. Vene and D. Hadzi, J. Chem. Phys. **49**, 4996 (1968).

[12] E. Rapoport, J. Chem. Phys. 53, 311 (1970).

[13] J. Grunberg, S. Levin, I. Pelah and D. Gerlich, Phys. Stat. Sol. (b) **49**, 857 (1972).

[14] L. P. Pereverzeva, N. Z. Pogosskaya, Yu. M. Poplavko,V. I. Pakhomov, I. S. Rez and G. B. Sil'nitskaya, Soviet Phys. Solid State **13**, 2690 (1972).

[15] R. A. Dalterio and F. J. Owens, J. Phys. C **21**, 6177 (1988).

[16] A. I. Baranov, V. P. Khiznichenko and L. A. Shuvalov, Ferroelectrics **100**, 135 (1989).

[17] K. S. Lee, J. Phys. Chem. Solids **57**, 333 (1996).

[18] B. K. Choi, J. Phys. Chem. Solids **56**, 1023 (1995).

[19] T. Mhiri and P. H. Colombian, *Solid State Ionic*, **44** (1991) 235.

[20] J.-H. Park, B.-C, Choi, *Material Letters* **57(**2003) 2162.

[21] K. Funke, R. D. Banhatti, *Solid State Ionics* **169** (2004) 1.

[22] K. Funke, R. D. Banhatti, *Solid State Ionics* **177** (2006) 1551.

[23] V. D Noto, M. Vittadello, *Soli State Ionics* **147** (2002) 309.

[24] S. Kim, H. B. Park, J. W. Rhim, Y.M. Lee, *Solid State Ionics* **176** (2005) 117.

[25] V. Di Noto, M. Vittadello, S. Lavina, M. Fauri, S. Bizcasso, *J. Phys. Chem.* B **105** (2001) 4584.

[26] E. J. Murphy*, J. Appl.Phys*, **35**. 2609(1964).

[27] C. T. Perrino And P. Wentercek*, J. Solid State Chem*.,**17**. 121(1976).

[28] A. K. Jonscher, Dielectric Relaxation in Solids, Chelsia Dielectric Press, London, 1983.

[29] D. P. Almond, A. R. West, Nature (Lond.) **306** (1983) 456.

[30] P. B. Macedo, C. T. Moynihan, R. Bose, Phys. Chem.Glasses **13** (1972) 171.

[31] C. T. Moynihan, L. P. Boesch, R. Bose, Phys. Chem.Glasses **14** (1973) 122.

[32] S. R. Elliott, J. Non-Cryst. Solids 170 (1994) 97; J. C. Dyre, J. Non-Cryst. Solids **153** (1991) 219.

[33] K. L. Ngai, C. T. Moynihan, MRS Bull. **23** (1998) 51.

[34] I. M. Hodge, K.L. Ngai, C.T. Moynihan, J. Non-Cryst. Solids **351** (2005) 104.

[35] G. Williams and D. C. Watts, Trans. Faraday Soc., 170, 66, 80.

[36] G. Williams and D. C. Watts, Trans. Faraday Soc., **67** (1971) 1323.

[37] P. B. Macedo, C. T. Moynihan, R. Bose, Phys. Chem.Glasses **13** (1972) 171.

[38] C. T. Moynihan, L. P. Boesch, R. Bose, Phys. Chem.Glasses **14** (1973) 122.

[39] K. L. Ngai, in: R. Richert and A. Blumen (eds.), *Effects of disorder on relaxation processes*, Springer-Verlag, Berlin, 1994.

[40] N. F. Uvarov, B. B. Bohonov, V. P. Isupov and E. F. Hairetdinov*, Solid State Ionics*, **74** (1994) 15.

[41] V. G. Ponomareva, G. V. Lavrova and L. G. Simonova, *Solid State Ionics*, **118** (1999) 317.

[42] T. Mhiri and P. H. Colombian, *Solid State Ionic*, **44** (1991)235.

[43] L. B. Harris and G. L. Vella. *J. Chem.Phys*, **58**. 4550(1972).

[44] A. A. Assencia and C. Mahadevan, *Bull, Mater. Sci.,* Vol. **28** No. 5, (2005) 415.